

## Real-Time Observation of Nonadiabatic Surface Dynamics: The First Picosecond in the Dissociation of NO on Iridium

Ian M. Lane,<sup>1</sup> David A. King,<sup>1</sup> Zhi-Pan Liu,<sup>2</sup> and Heike Arnolds<sup>1</sup>

<sup>1</sup>*Department of Chemistry, University of Cambridge, Lensfield Road, Cambridge CB2 1EW, United Kingdom*

<sup>2</sup>*Shanghai Key Laboratory of Molecular Catalysis and Innovative Materials, Department of Chemistry, Fudan University, Shanghai, 200433, People's Republic of China*

(Received 10 August 2006; published 3 November 2006)

Ultrafast laser pulses on Ir{111} cause a highly temperature-dependent redshift of the intramolecular stretch frequency of adsorbed NO. The time-resolved spectral changes are driven by charge transfer of hot electrons to the NO  $2\pi^*$  antibonding orbital, which leads to bending of NO and internal bond weakening. The nonadiabatic change in the NO adsorption geometry follows the charge transfer within a time scale of 700 femtoseconds. This geometrical change is the same as the mechanism predicted for thermally induced dissociation.

DOI: [10.1103/PhysRevLett.97.186105](https://doi.org/10.1103/PhysRevLett.97.186105)

PACS numbers: 68.35.Ja, 78.47.+p, 82.20.Gk, 82.53.St

The breaking and making of chemical bonds is central to surface catalysis. The time it takes reactants to rearrange into products is merely of the order of a few hundred femtoseconds. While direct detection of nuclear dynamics has only recently become feasible with the development of ultrafast electron diffraction [1], ultrafast vibrational spectroscopy has provided us with fascinating insights into adsorbate dynamics.

In particular, infrared-visible sum frequency generation (SFG) has been a powerful tool in disentangling the electron and phonon-driven contributions to the dynamics of desorption [2–4] and, most recently, diffusion [5]. In this Letter, we address the ultrafast dynamics of another key step in surface catalysis—dissociation. We monitor nitric oxide, whose rich surface chemistry [6] has received much recent attention with a view to reducing pollution from vehicle emissions [7,8]. We report on the femtosecond dynamics of NO on the iridium {111} surface and demonstrate, in combination with density functional theory (DFT), how the observed spectral transients relate to hybridization between the iridium  $d_{z^2}$  and the NO  $2\pi^*$  orbital. This induces N-O bond weakening and ultimately dissociation.

For our experiments we used an Ir{111} surface in an ultrahigh vacuum chamber and dosed a saturation coverage of NO corresponding to one NO per two Ir surface atoms. At this coverage NO molecules sit on atop, bridge, and hollow sites [9,10]. Using broadband SFG, we detect the atop molecules at a N-O stretching frequency of  $1860\text{ cm}^{-1}$ . NO adsorbed on hollow and bridge sites is known to have frequencies of  $1440\text{ cm}^{-1}$  and  $1550\text{ cm}^{-1}$ , respectively, but signal from these sites was below our detection limit for SFG. Presence of the low-frequency NO species prevents ultimate dissociation of the atop species through site blocking [6], ensuring that the NO adlayer remains stable from pulse to pulse.

For the visible pump-SFG probe spectroscopy we used a 10 Hz amplified Ti:sapphire system at 800 nm with a pulse

width of 150 fs. Part of the output is converted to infrared in an optical parametric amplifier, part is spectrally shaped to produce 4 ps 800 nm pulses for SF up-conversion, and the rest is used as a pump beam (absorbed fluence between 1 and  $15\text{ J m}^{-2}$ ). All three beams are overlapped noncollinearly on the surface at an average incidence angle of  $60^\circ$  and a spot size of approximately  $300\text{ }\mu\text{m}$  for the SFG beams and 1 mm for the pump beam.

Figure 1 shows the changes to the N-O stretch frequency and linewidth of a saturated layer at 100 K base temperature as a function of pump-probe time delay. These spectra show a very fast change within  $\pm 2\text{ ps}$  of zero time delay and a slower recovery on a time scale of tens of picoseconds. The frequency shifts to the red by maximally  $12\text{ cm}^{-1}$  while the linewidth more than doubles from around  $8\text{ cm}^{-1}$  to nearly  $20\text{ cm}^{-1}$ .

The two observed time scales are clearly reminiscent of the disequilibrium between electrons and phonons, caused by the fast energy input from the pump laser and the low heat capacity of the metal electrons, as shown in the inset to Fig. 1.

The transients in Fig. 2 demonstrate that the magnitude of the fast change strongly depends upon pump fluence, indicative of adsorbate interactions with the hot metal electrons. At low fluence, the N-O frequency follows the phonon temperature, while at higher fluence, perturbation of the N-O bond by the metal electrons is extremely pronounced. This large change from phonon to electronlike character is unlike any reported fluence dependence for adsorbed CO [2,11]. Pump wavelengths of 400 nm or 1590 nm have the same effect as 800 nm, provided the fluence is kept constant. This suggests that direct resonant excitation by nascent electrons does not contribute to the transients.

Modeling of such pump-probe data was previously based around the two-temperature model for describing the equilibration between electrons and phonons (respective temperatures  $T_{\text{el}}$  and  $T_{\text{lat}}$  shown in the inset to Fig. 1)

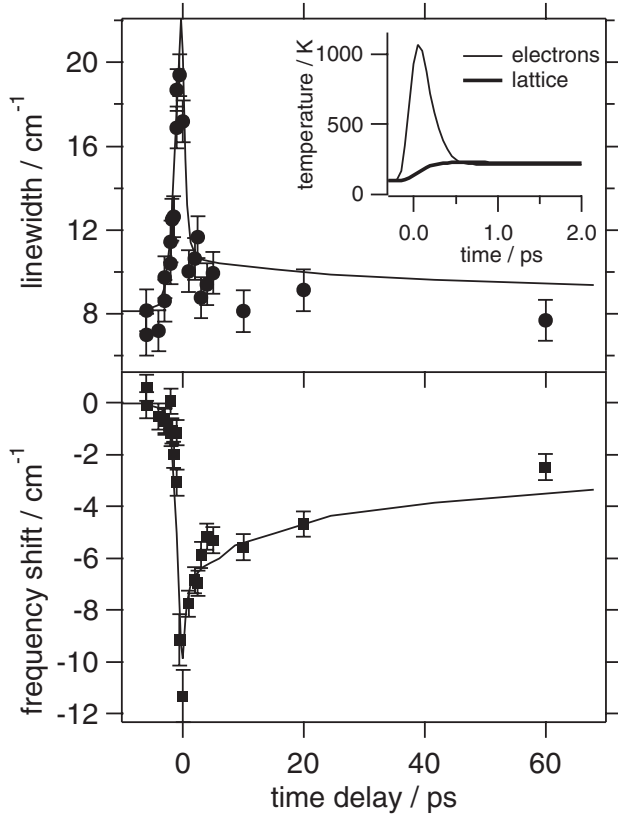


FIG. 1. Measured and calculated time-dependent NO frequency shifts and linewidths for an 800 nm, 150 fs pump pulse with  $10 \text{ J m}^{-2}$  absorbed fluence. Also shown are calculated time-dependent electron and lattice temperatures.

[12,13]. The transient frequency change is assumed to have the same origin as the commonly observed redshift with increasing surface temperature. This has been explained by anharmonic coupling of the high frequency stretch with a low-frequency mode, like the frustrated translation at  $\sim 60 \text{ cm}^{-1}$ . A fast transient can be generated by either coupling the frustrated translation to the hot electrons (typically on a time scale of a few picoseconds) or by adding the frustrated rotation as a second mode which separately couples to the electrons [4,5]. This approach could describe our transients, but only if we assumed a strong temperature dependence of the coupling time. Specifically, the electron coupling time would have to decrease by a factor ten for the fluence range shown in Fig. 2. While such a phenomenological description establishes the importance of these low-frequency modes, we aim to gain a deeper insight into the physical mechanism behind these observations.

To this end we devise a new model, which incorporates a specific coupling mechanism. The model is based on electronic friction and underpinned by DFT, and naturally incorporates the fluence-dependent changes we observe. We begin with the premise that hot electrons can lead to a transient increase in the occupation of the NO  $2\pi^*d$  anti-

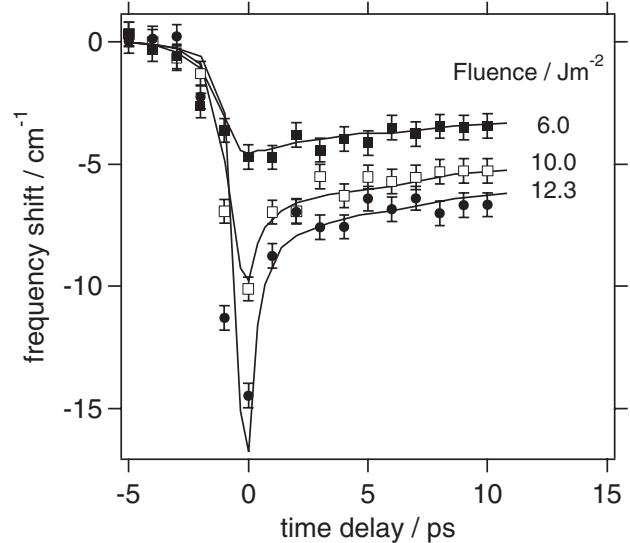


FIG. 2. Frequency transients for absorbed fluences of  $6 \text{ J m}^{-2}$ ,  $10 \text{ J m}^{-2}$ , and  $12.3 \text{ J m}^{-2}$ . Solid lines have been calculated according to the model described in the text.

bonding orbital. In traditional metal nitrosyl chemistry this charge transfer leads to a bent MNO group [14] and pronounced redshift of the N-O frequency [15]. These effects are extremely sensitive to charge transfer, as a second electron in the  $2\pi^*d$  orbital shifts the frequency by about  $500 \text{ cm}^{-1}$ .

On the iridium surface, bending of NO entails a change from upright bonding, where the metal's  $d_{z^2}$  orbital mixes with the NO  $5\sigma$  orbital, to a bent configuration with additional hybridization with the NO  $2\pi^*$  orbital. This increases the backdonation from the metal to the adsorbate.

The increased backdonation caused by femtosecond laser excitation was first described by Brandbyge *et al.* in terms of electronic friction [16]. They proposed that direct energy transfer between the metal electrons and adsorbate motion occurs via charge transfer to the adsorbate  $2\pi^*d$  resonance. The overlap between the metal Fermi distribution and the adsorbate orbital can be strongly temperature dependent, controlled by the resonance position and width (Fig. 3).

The NO  $2\pi^*d$  antibonding orbital lies between 1.3 and 1.6 eV above the Fermi level ( $E_f$ ), as measured by inverse photoemission on a number of transition metal surfaces [17,18]. Our DFT calculation places the NO  $2\pi^*d$  orbital 1.5 eV above  $E_f$  for the Ir{111} surface [19]. This is more accessible to hot electrons than CO, where the  $2\pi^*d$  orbital is typically 3 eV above the Fermi level. The first confirmation of our model is that fluence-dependent experiments for adsorbed CO show no fast transients [20].

We model our pump-probe data by assuming that the adsorbate frequency shift is composed of two components: one derives from those times when electrons and lattice are in equilibrium (thermal component  $\nu_{\text{lat}}$ ); the other origi-

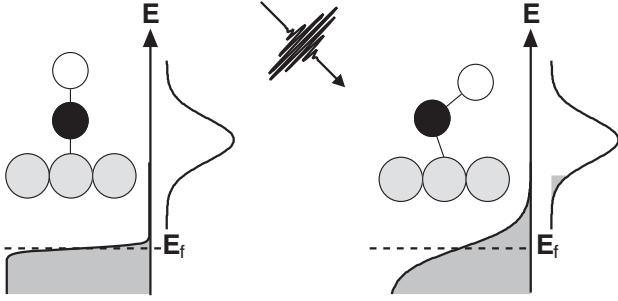


FIG. 3. A schematic diagram showing the thermalized hot Fermi-Dirac electron distribution after excitation with a femto-second optical pulse. The greater density of hot electrons can populate the adsorbate  $2\pi^*d$ , causing bending of the NO molecule.

nates from hot electrons ( $\nu_{el}$ ):

$$\nu(t) = \nu_{lat}(t) + \nu_{el}(t). \quad (1)$$

We calculate the thermal component  $\nu_{lat}$  using the statically measured linear temperature dependence with gradient  $\xi = 0.05 \text{ cm}^{-1}/\text{K}$  and frequency  $\omega_0 = 1860 \text{ cm}^{-1}$  at 100 K:

$$\nu_{lat}(t) = \omega_0 - [T_{lat}(t) - 100 \text{ K}]\xi. \quad (2)$$

The magnitude of the electronic contribution is given by the overlap between the Fermi distribution  $n_f(\epsilon)$  and the unoccupied  $2\pi^*d$  adsorbate orbital  $\Pi_{ads}$ . The degree of overlap  $A(T_{el})$  increases as the electron temperature rises and the Fermi distribution broadens. The time scale of the electronic contribution is given by  $\tau_{el}$ , which is the time it takes for the NO to bend in response to increased population of the  $2\pi^*d$  orbital.  $\tau_{el}$  can be thought of as the nonadiabaticity of the system. We therefore have

$$\frac{d\nu_{el}(t)}{dt} = -A(T_{el}) + \frac{1}{\tau_{el}} \nu_{el}(t), \quad (3)$$

$$A(T_{el}) = \beta \int_{-\infty}^{\infty} n_f(\epsilon, T_{el}) \Pi_{ads}(\epsilon) d\epsilon, \quad (4)$$

where  $\beta$  converts the degree of overlap into a frequency shift. This conversion factor depends on how many electrons are available [ $N(E_f) \sim 1e^-/\text{atom}/\text{eV}$ ] [21], the time scale of electron arrival ( $t_r \sim 10^{-13} \text{ s}$ ), and the relationship between  $2\pi^*d$  occupancy and frequency ( $\varpi \sim 500 \text{ cm}^{-1}/e^-$ ) [15].

$$\beta = \frac{N(E_f)\varpi}{t_r} = 5 \times 10^{18} \text{ cm}^{-1} \text{ s}^{-1}. \quad (5)$$

The adsorbate orbital  $\Pi_{ads}$  is modeled as a Gaussian, at a fixed level of 1.5 eV above  $E_f$  given by DFT. The instantaneous frequency changes  $\nu_{el}(t)$  and  $\nu_{lat}(t)$  are then used as an input to the optical Bloch equations in order to fit the data. The parameters varied are the FWHM of the  $2\pi^*d$  orbital,  $\beta$  and  $\tau_{el}$ .

Together with the frequency changes, we model the instantaneous linewidth changes as a sum of thermal and electronic components. The thermal component is given by the extrapolated static temperature dependence of the linewidth. There is no *a priori* way to predict the electronic component of the linewidth, but we can account qualitatively for the observed increase within the electronic friction framework. Tully *et al.* [22] explain the short vibrational lifetime of the internal molecular stretch by charge transfer during one oscillation of the N-O bond. Bending of NO moves the molecule's center of mass closer to the surface, thereby increasing this contribution. A quantitative estimate is beyond the scope of the present work.

The new model gives excellent agreement with our data. Solid lines in Figs. 1 and 2 use  $\beta = 8 \times 10^{16} \text{ cm}^{-1} \text{ s}^{-1}$ , an orbital FWHM of 0.70 eV, and a coupling constant of 700 fs. The charge transfer contribution to the data in Fig. 1 is  $10 \text{ cm}^{-1}$ , which corresponds to 0.02 electrons, based on the known gradient for metal nitrosyls.

In corroboration of our model, we have carried out DFT calculations to show that a bent adsorption geometry for NO/Ir{111} leads to a comparable redshift of the NO frequency [19]. The relative energy of this bent state is calculated with respect to the relaxed upright state, as well as the optimized Ir-N-O angle, NO frequency, and electron gain.

DFT calculations find that atop NO is upright with an Ir-N-O angle of  $178^\circ$ , an N-O distance of 1.176 Å, and an N-Ir distance of 1.760 Å. At an Ir-N-O angle of  $159^\circ$ , the N-O distance increases to 1.181 Å, the N-Ir distance expands to 1.785 Å, and the total energy of the system increases by  $\Delta E = 0.14 \text{ eV}$ , as shown in Fig. 4. At the largest angle, the calculated N-O frequency has dropped by  $54 \text{ cm}^{-1}$ , which fits very well with our experimental results, given that SFG integrates fast changes over the inverse linewidth [13], which we measured as 1.5 ps from a free induction decay [3].

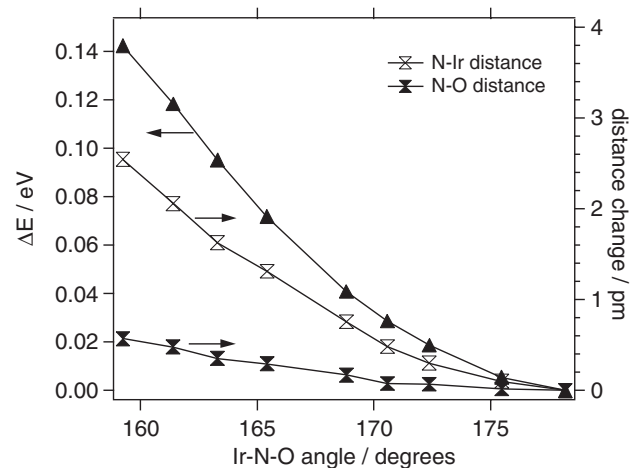


FIG. 4. Energy increase and changes in N-O and N-Ir distance as a function of the Ir-N-O angle.

The calculated total electron gain for NO, which derives solely from increased  $2\pi^*d$  occupation, is  $0.03e^-$  in this case. This is excellent confirmation of our basic assumption that bent adsorbed NO and increased  $2\pi^*d$  occupation are intimately connected.

From comparison with DFT, we can estimate that at the highest fluence shown in Fig. 2, where the electron temperature reaches around 1200 K ( $=0.1$  eV), the molecular axis is at a  $15^\circ$  angle with respect to the surface normal. At the same time, the nitrogen atom is shifted away from the center of the metal atom. As a consequence, both N-O and N-Ir bonds are longer and therefore weaker. NO bending follows the electron temperature with a nonadiabatic coupling time of 700 fs. The bending motion is akin, but not identical to, the standard frustrated rotational mode, as it involves a change in the orbital hybridization involved in bonding. The bending and concomitant N-O and N-Ir bond lengthening would, however, explain the high rotational and vibrational temperatures typically observed in fs laser-desorbed NO [23,24].

Our results have a strong bearing on thermal NO surface chemistry. There, the key factor in the propensity of NO to dissociate is the position of the metal  $d$  band with respect to the NO  $2\pi^*$  orbital. An increased overlap strengthens the NO-metal bond and weakens the internal N-O bond, putting iridium at the borderline between dissociative and molecular adsorption [6]. With the help of a femtosecond pump pulse, we are briefly increasing the overlap between electrons and  $2\pi^*d$  antibonding orbital, which is observable as weakening of the internal bond. From our experimental results we can deduce that less than an extra tenth of an electron is required to strongly bend the NO, thereby promoting dissociation. From this we predict that Ir is an ideal surface to test how far NO dissociation can be controlled through alloying, which changes the position of the  $d$ -band center [25].

Our results provide us with the first real glimpse of NO dissociation. The pathway calculated by DFT involves bending in an entirely analogous fashion to the motion on the atop site [19,26]. The DFT minimum energy route starts from the hollow site, while experiments indicate that NO adsorbed on atop sites dissociates at low coverage on iridium [9,27]. We consider the bending motion from the atop site a viable path to dissociation, of which we monitor the first picosecond.

In conclusion, we have observed a strong nonadiabatic coupling between iridium electrons and adsorbed NO at a time scale of 700 fs. The origin is increasing backdonation from the hot metal  $d$  electrons to the adsorbate  $2\pi^*d$  antibonding orbital. This causes bending of NO and internal bond weakening and is noted to be the first step towards dissociation.

We are grateful to EPSRC for equipment funding and financial support for I.M.L. and support from Toyota Motor Inc. for H. A.

- [1] C. Y. Ruan, F. Vigliotti, V. A. Lobastov, S. Y. Chen, and A. H. Zewail, Proc. Natl. Acad. Sci. U.S.A. **101**, 1123 (2004).
- [2] M. Bonn, C. Hess, S. Funk, J. H. Miners, B. N. J. Persson, M. Wolf, and G. Ertl, Phys. Rev. Lett. **84**, 4653 (2000).
- [3] J. P. R. Symonds, H. Arnolds, and D. A. King, J. Phys. Chem. B **108**, 14 311 (2004).
- [4] F. Fournier, W. Q. Zheng, S. Carrez, H. Dubost, and B. Bourguignon, J. Chem. Phys. **121**, 4839 (2004).
- [5] E. H. G. Backus, A. Eichler, A. W. Kleyn, and M. Bonn, Science **310**, 1790 (2005).
- [6] W. A. Brown and D. A. King, J. Phys. Chem. B **104**, 2578 (2000).
- [7] Z. P. Liu, S. J. Jenkins, and D. A. King, J. Am. Chem. Soc. **126**, 10 746 (2004).
- [8] Z. P. Liu, S. J. Jenkins, and D. A. King, J. Am. Chem. Soc. **125**, 14 660 (2003).
- [9] J. C. L. Cornish and N. R. Avery, Surf. Sci. **235**, 209 (1990).
- [10] M. Gajdos, J. Hafner, and A. Eichler, Journal of Physics-Condensed Matter **18**, 13 (2006).
- [11] J. P. Culver, M. Li, Z. J. Sun, R. M. Hochstrasser, and A. G. Yodh, Chem. Phys. **205**, 159 (1996).
- [12] T. A. Germer, J. C. Stephenson, E. J. Heilweil, and R. R. Cavanagh, J. Chem. Phys. **98**, 9986 (1993).
- [13] S. Roke, A. W. Kleyn, and M. Bonn, J. Phys. Chem. A **105**, 1683 (2001).
- [14] W. Evans and J. Zink, J. Am. Chem. Soc. **103**, 2635 (1981).
- [15] R. Fenske and R. DeKock, Inorg. Chem. **11**, 437 (1972).
- [16] M. Brandbyge, P. Hedegard, T. F. Heinz, J. A. Misewich, and D. M. News, Phys. Rev. B **52**, 6042 (1995).
- [17] P. D. Johnson and S. L. Hulbert, Phys. Rev. B **35**, 9427 (1987).
- [18] I. Kinoshita, A. Misu, and T. Munakata, J. Chem. Phys. **102**, 2970 (1995).
- [19] Total energy calculations were performed using the DFT-slab approach with a GGA-PBE functional, implemented with the program CASTEP. The Ir{111} surface was modeled by a four-layer slab with top layer relaxed;  $x$  and  $y$  are coordinates within the surface layer. To mimic the effect a bending of the Ir-N-O group would have on the N-O stretch frequency, the  $y$  coordinate of the oxygen atom is fixed at various positions, while all other parameters are allowed to relax.
- [20] I. M. Lane, Z. P. Liu, D. A. King, and H. Arnolds (to be published).
- [21] J. Noffke and L. Fritsche, Journal of Physics F-Metal Physics **12**, 921 (1982).
- [22] M. Head-Gordon and J. C. Tully, J. Chem. Phys. **96**, 3939 (1992).
- [23] T. Yamanaka, A. Hellman, S. W. Gao, and W. Ho, Surf. Sci. **514**, 404 (2002).
- [24] F. Budde, T. F. Heinz, A. Kalamirides, M. M. T. Loy, and J. A. Misewich, Surf. Sci. **283**, 143 (1993).
- [25] B. Hammer and J. K. Norskov, Surf. Sci. **343**, 211 (1995).
- [26] M. Gajdos, J. Hafner, and A. Eichler, Journal of Physics-Condensed Matter **18**, 41 (2006).
- [27] J. E. Davis, S. G. Karseboom, P. D. Nolan, and C. B. Mullins, J. Chem. Phys. **105**, 8362 (1996).